Comparative Static and Rapid Load Tests on Steel Pipe Piles: A Case Study at Sashima Test Yard

Shihchun Lin, Koji Watanabe, Shuichi Kamei, and Tatsunori Matsumoto

Abstract To obtain the load–displacement curve of a pile, static load test (SLT), dynamic load test (DLT) and rapid load test (RLT) are generally used. In this research, SLT and RLTs on two open-ended steel pipe piles (SPPs) were carried out in the Jibanshikenjo test yard at Sashima, Ibaraki Prefecture. The test piles had an outer diameter of 318.5 mm, a wall thickness of 6.6 mm and an embedment length of 11.0 m. The ground at the test site is alternative layers of sand, clay and silt having SPT N-values less 35. In the RLTs, relative loading duration T_r was intentionally varied in a range from 3 to 5. Static load–displacement curves obtained from various interpretation methods of RLT signals are compared with the load–displacement curve directly obtained from SLT to examine the applicability of each interpretation method.

Keywords Rapid load test · Static load test · Steel pipe pile · Interpretation method · Case study

S. Lin (✉) · S. Kamei
Jibanshiknjo Co. Ltd, Tokyo, Japan
e-mail: s_rin@mail.jibanshikenjo.co.jp

S. Kamei
e-mail: s_kamei@mail.jibanshikenjo.co.jp

K. Watanabe
Aichi Institute of Technology, Nagoya, Japan
e-mail: k-watanabe_28@aitech.ac.jp

T. Matsumoto
Kanazawa University, Kanazawa, Japan

P. Duc Long and N. T. Dung (eds.), *Proceedings of the 5th International Conference on Geotechnics for Sustainable Infrastructure Development*, Lecture Notes in Civil Engineering 395, https://doi.org/10.1007/978-981-99-9722-0_18

1 Introduction

Twenty years have passed since the rapid load test (RLT) of piles was newly added to the Japan Geotechnical Society (JGS) standard (JGS1815-2002) [1]. In the dynamic load test (DLT), known as the PDA test, the soil resistance during driving can be estimated from the measured dynamic signals based on the one-dimensional stress-wave theory. To obtain a static load–displacement relation of the pile, wave matching analysis (WMA) needs to be conducted. The results of WMA depend on the soil resistance model used and the interpretation of the analyst [2]. The purpose of the RLT is the estimation of static load–displacement curve of the tested pile from a simplified interpretation of the measured dynamic signals. The ultimate bearing capacity is determined from the load–displacement curve depending on definition of the ultimate bearing capacity, e.g., pile head load at pile head displacement of 10% of the pile diameter.

After 2002, most of the RLTs in Japan are conducted using the falling-mass method with a soft cushion placed on the pile head. In line with this, the number of loading cycles has also changed from one loading (blow) with the maximum planned load to multiple blows with the hammer drop height being raised in stages. Therefore, the interpretation method has shifted from the unloading point (ULP) method to the unloading point connection (ULPC) method which provides a static load–displacement relationship simply by connecting the ULPs without the need to obtain the damping constant C required in the ULP method.

Kamei et al. [3] pointed out that the ULPC method, in which the pile is assumed as a rigid single mass, tends to overestimate the static pile resistance.

In this paper, static load–displacement relations of two steel pipe piles (SPPs) from static load tests (SLTs) and RLTs with two new interpretation methods, the ULPC method invoking the case method (ULPC_CM) [4] and segmental unloading point connect method (SULPC) [5], were compared to examine the advantages of the new interpretation methods over the conventional ULPC method.

2 Outline of Pile Load Tests

2.1 Site Conditions

Load tests were carried out in Sashima test yard of Jibanshikenjo Co. Ltd., Japan. Figure 1 shows the arrangements of soil investigations and test piles. One standard penetration test (SPT) and electric cone penetration tests (CPTs) were carried out at just points of test piles.

Figure 2 shows the results of soil investigations, and embedment of the instrumented test piles. SPT N-values from the ground level to a depth $z = 5$ m are 1 to 3. Below this depth, N-value increases with depth. Below $z = 10$ m, a sand layer with

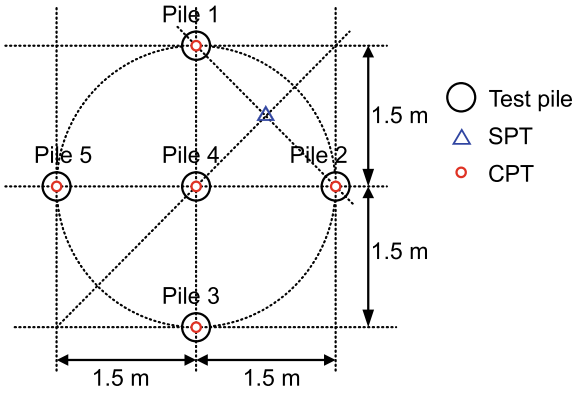

Fig. 1 Arrangements of SPT, CPTs and test piles

$N \approx 33$ exists. The test piles were driven to $z = 11$ m. Groundwater table is at $z = 3.5$ m.

It can be seen from the distributions of SPT N-values and CPT q_t (cone resistance corrected for pore pressure at filter) that ground conditions are similar in each test pile location.

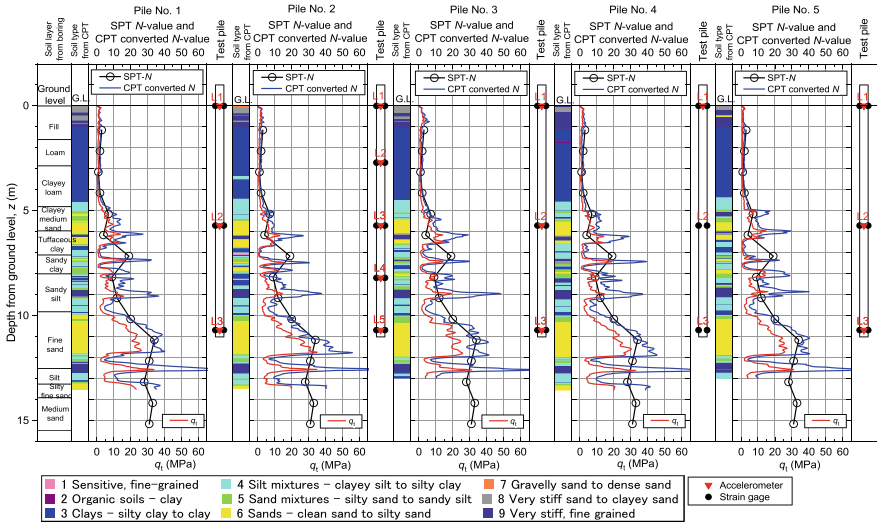

Fig. 2 Profiles of soil layers, SPT N-values and CPT q_t, together with instrumented test piles

Table 1 Specifications of test piles

Item	Value	
	Original	With protection
Pile length, L (m)	11.8	
Embedment length, L_d (m)	11.0	
Outer diameter, D_o (mm)	318.5	
Inner diameter, D_i (mm)	305.3	
Wall thickness, t_w (mm)	6.6	
Cross-sectional area, A (m^2)	0.00651	0.00926
Young's modulus, E (GPa)	205	
Density, ρ (ton/m^3)	7.81	
Bar wave velocity, c (m/s)	5123	
Mass, m (ton)	0.610	0.819

2.2 Test Piles

Table 1 shows the specifications of test steel pipe piles (SPPs). Channel steels were welded on the outer surface of the test SPPs for protecting strain gages and accelerometers. The specifications of the five test piles are the same.

2.3 Test Cases

Table 2 shows the test sequence of each test pile. Dynamic load tests (DLTs) were carried out during initial pile driving. After curing period of 1 day, DLTs were carried out again on Pile No. 1 and Pile No. 2 to grasp "setup" phenomena. RLTs with the relative loading duration $T_r = t_L/(2L/c) = 5$ (t_L is the loading duration) were carried out on Pile No. 1 and Pile No. 4, according to the JGS standards (JGS, 2002) in which $T_r \geq 5$.is required. RLTs with $T_r = 3$ were carried out on Pile No. 2 intentionally. If RLT with shorter T_r is reasonable, it will be possible to apply RLT to piles with longer length and greater bearing capacity using the current RLT devices.

3 Interpretation Methods

In this section, interpretation methods of RLT signals used in this research are described.

Table 2 List of test sequence

Pile no	Driving date (DLT)	Curing (day)	DLT	Curing (day)	Load test		Curing (day)	Load test	
1	2022/05/11	1	2022/05/12	30	RLT (T_r = 5)	2022/06/11	–	–	
2	2022/05/11	1	2022/05/12	33	RLT (T_r = 3)	2022/06/14	184	SLT	2022/12/15
3	2022/05/12	–	–	32	RLT (T_r = 4)	2022/06/13	–	–	
4	2022/05/12	–	–	25	SLT	2022/06/07	8	RLT (T_r = 5)	2022/06/15
5	2022/05/12	–	–	279	SLT	2023/02/15		RLT (under planning)	

3.1 ULPC Method

The ULPC method is an extension method of unloading point (ULP) method. In ULPC, the pile is treated as a single mass rigid body. To obtain soil resistance R_{soil}, the pile inertial force $R_{\text{a}} = m\,\alpha$(m = the pile mass and α = acceleration at pile head) is subtracted from the rapid load F_{rapid}. ULP is the point of R_{soil} at the maximum pile displacement w, where pile velocity $v = 0$. Hence, R_{soil} at ULP is equal to the static soil resistance R_w. By connecting ULPs from multiple blows, static load–displacement relation is easily obtained.

3.2 ULPC_CM Method [4]

The case method [6] is a method based on the one-dimensional stress-wave theory, in which the penetration resistance R_t ($= R_{\text{soil}}$) of a pile during driving is estimated.

First, the downward traveling wave F_d and the upward traveling wave F_u are calculated from the measured dynamic signals (axial force F and pile velocity v) by means of Eqs. (1) and (2), respectively. Then, by using Eq. (3), the time variation of R_t ($= R_{\text{soil}}$) is obtained (Fig. 3).

$$F_{\text{d}}(x_{\text{m}}, t) = \frac{F(x_{\text{m}}, t) + Z \cdot v(x_{\text{m}}, t)}{2} \tag{1}$$

$$F_{\text{u}}(x_{\text{m}}, t) = \frac{F(x_{\text{m}}, t) - Z \cdot v(x_{\text{m}}, t)}{2} \tag{2}$$

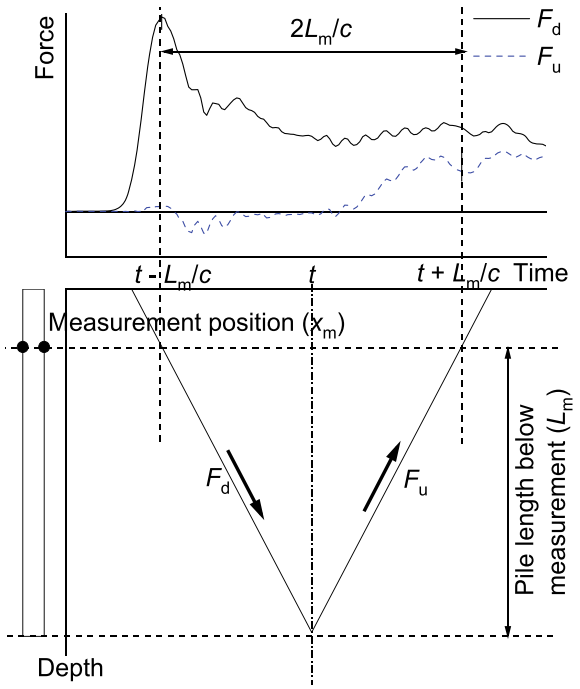

Fig. 3 Case method [6]

$$R_{\mathrm{t}}(x_{\mathrm{m}}, t) = F_{\mathrm{d}}\left(x_{\mathrm{m}}, t - \frac{L_{\mathrm{m}}}{c}\right) + F_{\mathrm{u}}\left(x_{\mathrm{m}}, t + \frac{L_{\mathrm{m}}}{c}\right) \tag{3}$$

Here, x = coordinate along the pile axis (pile head = 0), x_m = measurement position, v = pile velocity, L_m = pile length from x_m to pile tip, F = axial force, F_d = downward force wave, F_u = upward force wave, Z = impedance ($= EA/c$), c = bar wave velocity, E = Young's modulus of pile, A = cross-sectional area of pile.

The case method evaluates the penetration resistance of the pile during driving, but the load–displacement relationship of the pile cannot be obtained by this method alone. Since the case method is based on the one-dimensional wave theory, the penetration resistance of the pile can be evaluated correctly regardless of the pile length.

In the ULPC_CM method, multiple blows (rapid load tests) are applied to a pile. The time variation of soil resistance R_{soil} is obtained from the case method, and the time variation of pile displacement w is directly measured. Hence, R_{soil}–w relation is easily obtained. R_{soil} at the maximum pile displacement can be regarded as the static resistance R_w. Similar to the ULPC method, static load–displacement curve is constructed by connecting ULPs from the multiple blows.

As the ULPC_CM method is based on the one-dimensional stress-wave theory, it has the advantage of not requiring correction for pile inertia. Hence, the ULPC_CM method would be applied to RLTs on piles with $T_r < 5$.

3.3 SULPC Method [5]

Mullins et al. [7] proposed the segmental unloading point (SULP) method for a pile instrumented at several pile sections. In the SULP method, force and acceleration are measured at the pile head whereas only force is measured at other pile sections. The velocity and acceleration at a particular measurement point other than the pile head are estimated using the measured force at that point, and the force and displacement at the pile head. Note that only the total static soil resistance is estimated in the SULP method by summing up the static soil resistance of each pile segment.

In the segmental unloading point connection (SULPC) method, forces and accelerations are measured at several sections of the pile (Fig. 4). Soil resistance $R_{\text{soil\_}i}$ versus displacement w_i of segment i is estimated using the relation of Eq. (5) (Step 2 in Table 3).

$$\begin{aligned} R_{\text{soil}i}(t) &= F_{\text{rapid}i}(t) - m_i \cdot \alpha_i(t) \\ &= F_{i-1}(t) - F_i(t) - m_i \cdot \alpha_i(t) \end{aligned} \tag{4}$$

As several blows are applied to the pile (Step 1), static soil resistance R_{w_i} versus w_i of segment i is constructed by connecting ULPs (Step 3).

The responses of the whole pile subjected to static pile head load are then calculated using a one-dimensional FEM (Fig. 5) (Step 4). In this calculation stage, the pile is treated as elastic, and non-linear soil resistance behavior estimated in Step 3 is considered at each pile node.

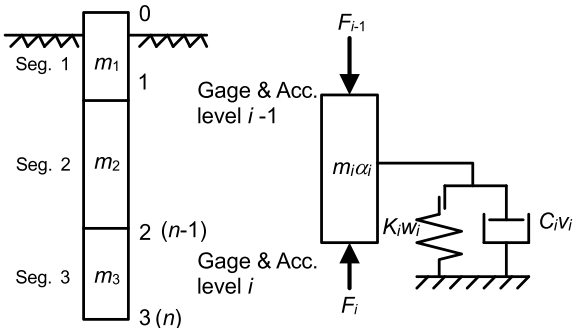

Fig. 4 Segmental unloading point connection (SULPC) method [5]

Table 3 Flow of SULPC

Step 1: Multicycle rapid load test
Step 2: Calculate relationship of soil resistance R_{soil}–displacement w and ULP load for each pile segment
Step 3: Construct static resistance R_w–displacement w relationship for each pile segment by connecting ULPs (SULPC)
Step 4: Analyze responses of elastic pile subjected to static loading using a load transfer method

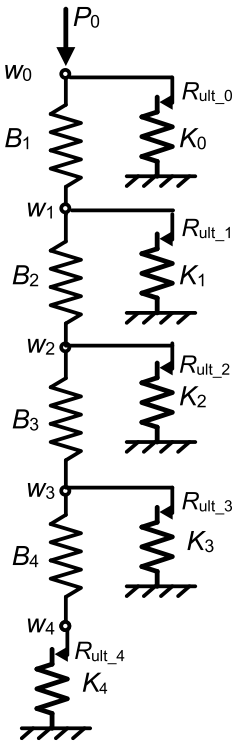

Fig. 5 One-dimensional FEM method

4 Load Test Results

4.1 SLT

SLTs were carried on Pile No. 4 and No. 2. The results of SLT will be shown in comparison with the RLT results later.

4.2 RLT (Pile No. 4)

In Pile No. 4, RLTs were carried out after SLT. In RLTs, a hammer mass $m_h = 3.5$ ton was used and eight blows (RLTs) were applied to the pile with increasing drop height h from 0.03 to 0.83 m. Loading duration t_L was adjusted by changing the stiffness of cushions placed on the pile head to have $T_r \geq 5$.

Figure 6 shows the measured dynamic signals, rapid load F_{rapid}, pile head displacement w, velocity v and acceleration α, in the RLT at $h = 0.83$ m. In the figure, soil resistance R_{soil} (ULPC) from the ULPC method and R_{soil} (ULPC_CM) from the

ULPC_CM method are shown together with F_{rapid}. Furthermore, F_d and F_u are also shown.

R_{soil} (ULPC_CM) at the maximum w where $v = 0$ is defined as the static resistance R_w (R_{ULP}) in a similar way to the ULPC method. Static load–displacement relation can be obtained by connecting R_{ULP} from ULPC_CM from multiple blows (RLTs).

Figure 7 shows the F_{rapid}, R_{soil} (ULPC) and R_w (ULPC) versus w from ULPC method. Figure 8 also shows the F_{rapid}, R_{soil} (ULPC_CM) and R_w (ULPC_CM) versus w from ULPC_CM method.

Comparing Figs. 7 and 8, R_{soil} (ULPC) is larger than R_{soil} (ULPC_CM). As [3] pointed out, this could be due to the excessive correction of the pile inertial force $m\alpha$ (where m is the pile mass including channel steel mass).

Figure 9 shows the R_w versus w of each pile segment from SULPC method. Pile No. 4 had three pile segments because dynamic measurements were made at three levels (L1 to L3) as shown in Fig. 2. The circles are the estimated values of each segment from multiple blows. The mobilization of R_w along each pile segment was

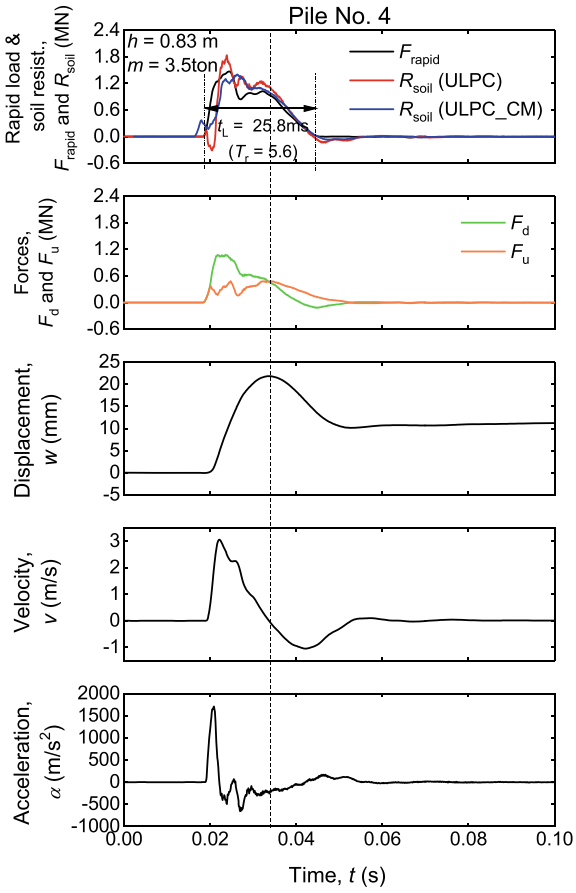

Fig. 6 RLT signals (Pile No. 4, $h = 0.83$ m)

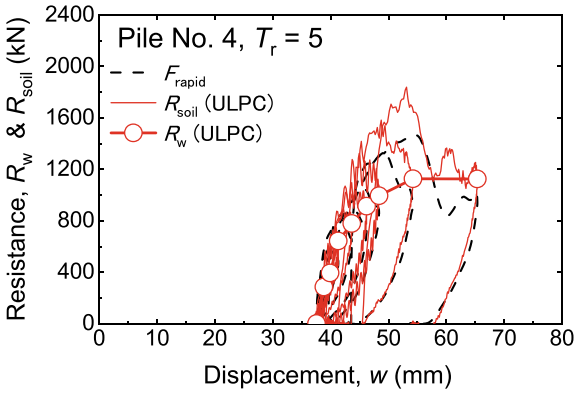

Fig. 7 F_{rapid}, R_{soil} and R_w versus w from ULPC (Pile No. 4)

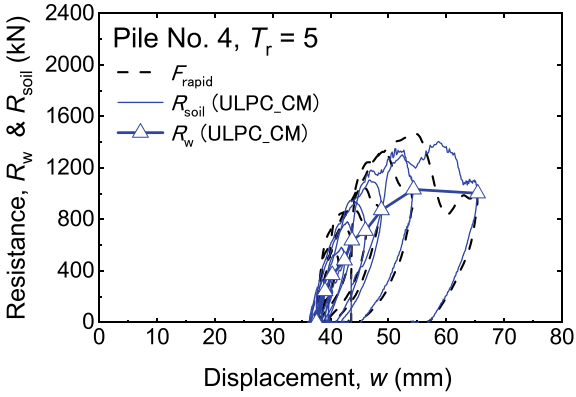

Fig. 8 F_{rapid}, R_{soil} and R_w versus w from ULPC_CM (Pile No. 4)

modeled as the dotted line, which was used in the one-dimensional FEM analysis of the pile response under static loading.

Figure 10 shows the static load–displacement relations from ULPC, ULPC_CM and SULPC compared with the SLT result. It is seen from the RLT results that the static soil resistance R_w from ULPC is larger than that from ULPC_CM. The load–displacement relation from ULPC_CM matches with the SLT result very well. The curve from SULPC is also comparable to the SLT result.

4.3 RLT (Pile No. 2)

In Pile No. 2, SLT was carried out after RLTs. In RLTs, a hammer mass $m_h = 0.95$ ton was used and 12 blows (RLTs) with $T_r = 3$ were applied to the pile with increasing drop height h from 0.02 to 3.84 m.

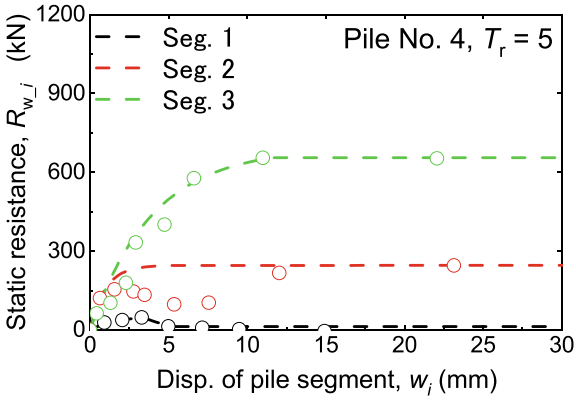

Fig. 9 R_w versus w of pile segments from SULPC method (Pile No. 4)

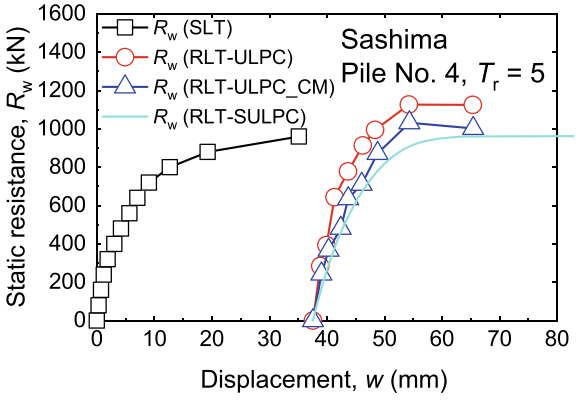

Fig. 10 Comparison of load–displacement curves from SLT, RLTs with ULPC, ULPC_CM and SULPC (Pile No. 4)

Figure 11 shows the measured F_{rapid}, w, v and α in the RLT in the eighth blow ($h = 1.35$ m) with $T_r = 3.2$. In the figure, R_{soil} (ULPC) and R_{soil} (ULPC_CM) are shown together with F_{rapid}. Furthermore, F_d and F_u are also shown.

Figure 12 shows the F_{rapid}, R_{soil} (ULPC) and R_w (ULPC) versus w from ULPC. Figure 13 also shows the F_{rapid}, R_{soil} (ULPC_CM) and R_w (ULPC_CM) versus w from ULPC_CM.

Comparing Figs. 12 and 13, R_{soil} (ULPC) is much larger than R_{soil} (ULPC_CM). The magnitude of acceleration α at the time instant of maximum pile displacement (ULP) of Pile No. 2 (Fig. 11) is much larger than that of Pile No. 4 (Fig. 6). Comparing with Fig. 7 (Pile No. 4), much larger R_{soil} (ULPC) than R_{soil} (ULPC_CM) is caused in Pile No. 2 by the excessive correction of the pile inertial force $m\alpha$.

Figure 14 shows the R_w versus w of each pile segment from SULPC method. Pile No. 2 had five pile segments because dynamic measurements were made at five levels (L1 to L5) as shown in Fig. 2.

Figure 15 shows the static load–displacement relations from ULPC, ULPC_CM and SULPC compared with SLT result. The load–displacement relation from ULPC_

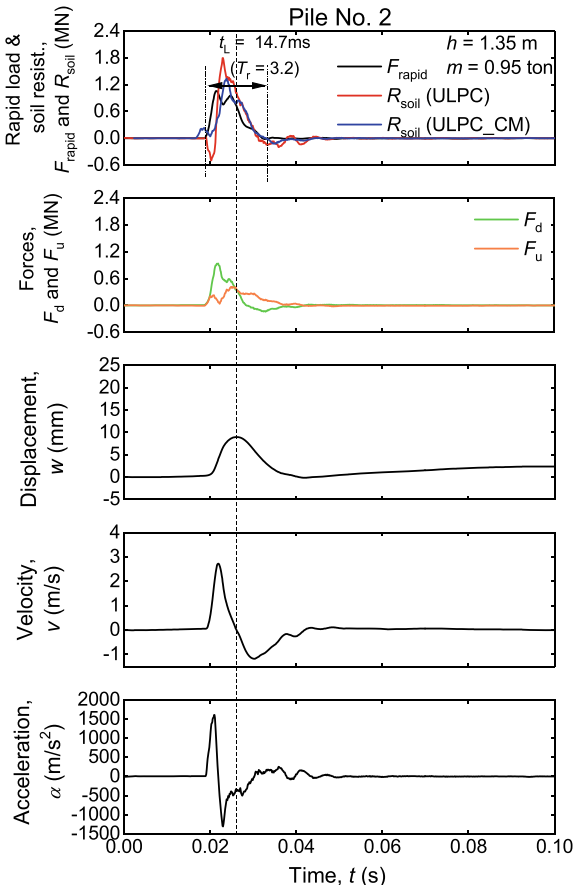

Fig. 11 RLT signals (Pile No. 2, $h = 1.35$ m)

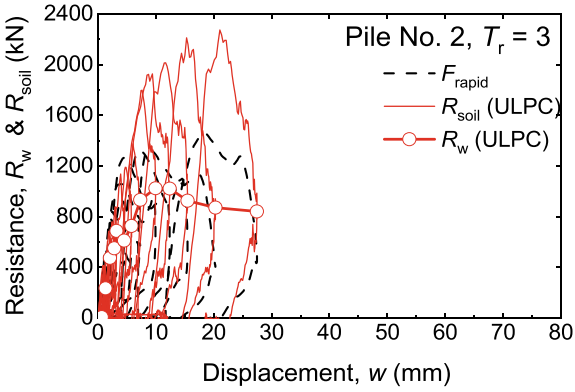

Fig. 12 F_{rapid}, R_{soil} and R_w versus w from ULPC (Pile No. 2)

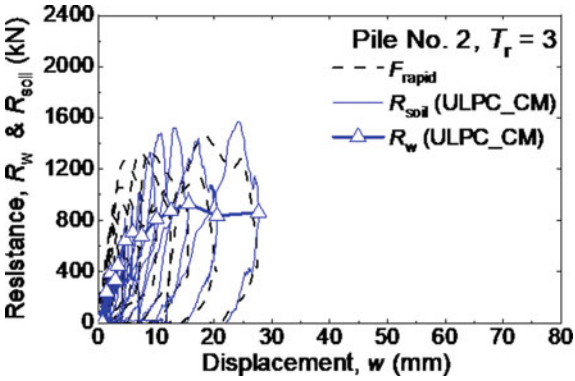

Fig. 13 F_{rapid}, R_{soil} and R_w versus w from ULPC_CM (Pile No. 2)

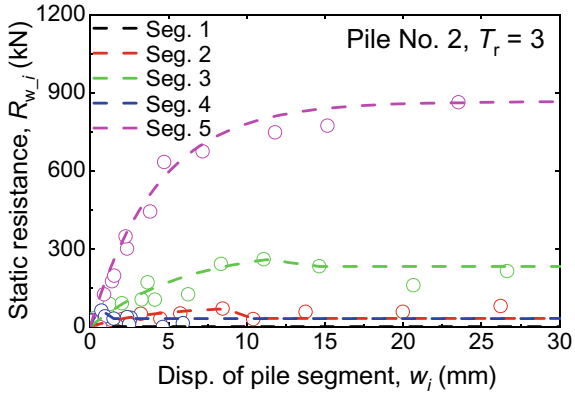

Fig. 14 R_w versus w from SULPC (Pile No. 2)

CM matches with the SLT result very well again, even for $T_r \approx 3$. The relation from SULPC also is a good estimation for the SLT result.

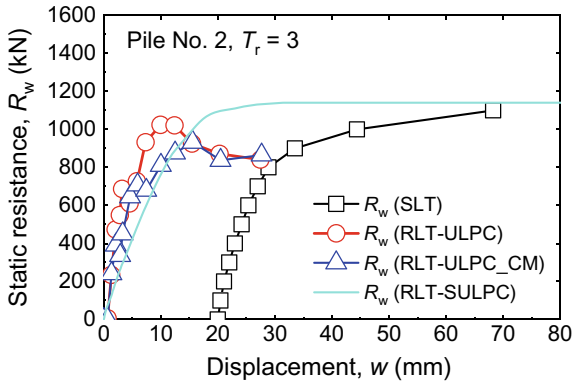

Fig. 15 Comparison of load–displacement curves from SLT, RLTs with ULPC, ULPC_CM and SULPC (Pile No. 2)

5 Conclusion

In this study, comparative RLTs and SLTs were carried out on driven steel pipe piles to examine the validity of the new interpretation methods, ULPC_CM and SULPC.

RLTs with $T_r = 5$ were carried out according to the JGS standards in which T_r is required to be greater than 5. Furthermore, RLTs with $T_r = 3$ were carried out with the aim of widening the application of RLT.

The static load–displacement relations from the ULPC_CM method and SULPC method matched with the SLT results very well even in cases of $T_r = 3$, regardless of order of SLT and RLT. In future, a similar comparison between RLTs and SLT with $T_r < 3$ will be needed to discuss the application limit of ULPC_CM method for RLTs with smaller T_r.

It can be said that it is possible to apply the RLT with ULPC_CM method or SULPC method to piles with longer length and greater bearing capacity using the current RLT devices.

The authors are planning to conduct similar comparisons between RLTs and SLT for different types of piles to examine the applicability of ULPC_CM method or SULPC method in the near future.

For comparison of the bearing capacities and the load–displacement curves estimated using the CPT and SPT data as well as the rapid pile load tests, refer to [8].

References

1. Japanese Geotechnical Society (JGS) (2002) JGS 1815–2002 Method for Rapid Load Test of Single Piles
2. Verbeek GHW, Bielefeld MW (2022) Alternative facts in pile testing. In: Proceeding of the 11th International conference on stress wave theory and design and testing methods for deep foundations, Rotterdam, The Netherlands. https://doi.org/10.5281/zenodo.7148281
3. Kamei S, Takano K, Fujita T (2022) Comparison of static load test and rapid load test on steel pipe piles in two sites. In: Proceeding of the 11th international conference on stress wave theory and design and testing methods for deep foundations, Rotterdam. https://doi.org/10.5281/zenodo.7148489
4. Lin S, Kamei S, Yamamoto I, Matsumoto T (2023a) Hybridnamic rapid load testing with UnLoading Point Connection method invoking Case method. In: Proceeding of the 17th Asian regional conference on Soil Mechanics and Geotechnical Engineering 2023, Nur-Sultan (accepted for publication).
5. Kamei S, Lin S, Yamamoto I, Matsumoto T (2023) Hybridnamic rapid load testing with an extended interpretation method of dynamic signals. In: Proceeding of the 17th Asian Regional Conference on Soil Mechanics and Geotechnical Engineering 2023, Nur-Sultan (Accepted for publication).
6. Raushe F, Goble G, Likins GE Jr (1985) Dynamic determination of pile capacity. ASCE J Geotech Div 111(3):367–383
7. Mullins G, Lewis LC, Justason MD (2002) Advancements in Statnamic data regression techniques. Proceeding of International Deep Foundations Congress 2002, Orlando

8. Lin S, Watanabe K, Kamei S, Naka Y, Matsumoto T (2023b) Load-displacement relations of a driven steel pipe piles from static and rapid load tests, and empirical formulas based on SPT and CPT: a case study at Sashima test yard. In: Proceeding of 5th international conference on geotechnics for sustainable infrastructure development, Hanoi (to be published)